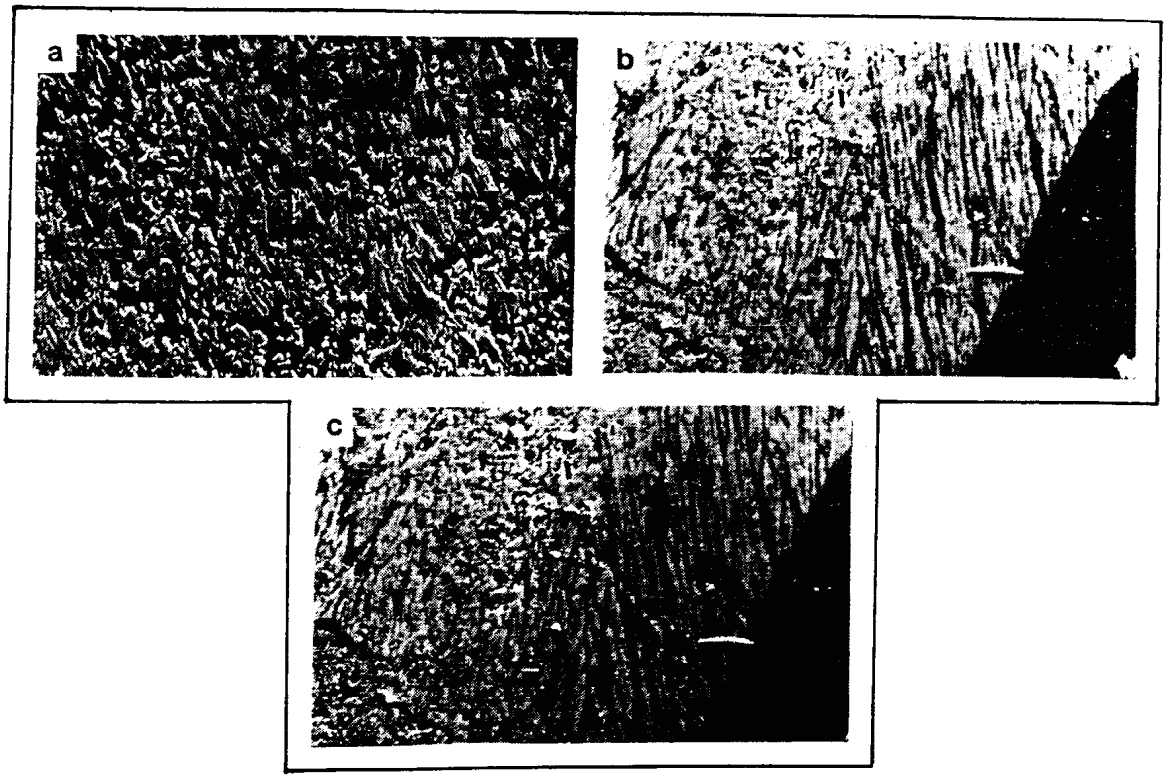

Figure 4.5 (ii) **Cross-sectional electron micrographs of the porous rim of a three hour leached Alloy C catalyst before WGSR**

a: MAG x 550
b: Zn mapping (MAG x 240)
c: Aℓ mapping (MAG x 240)

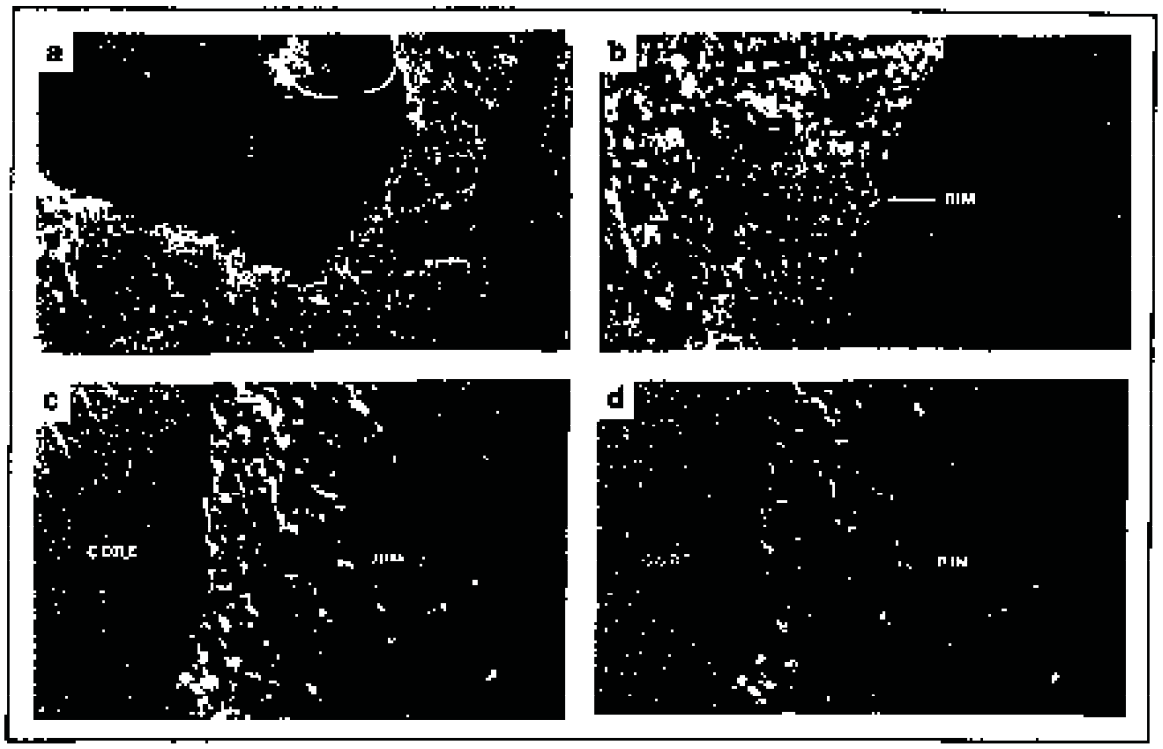

Figure 4.6 (i) Cross-sectional electron micrographs of the porous rim of a one hour leached Alloy C catalyst after WGSR

a: MAG x 220
b: MAG x 1000
c: Zn mapping (MAG x 550)
d: Al mapping (MAG x 550)

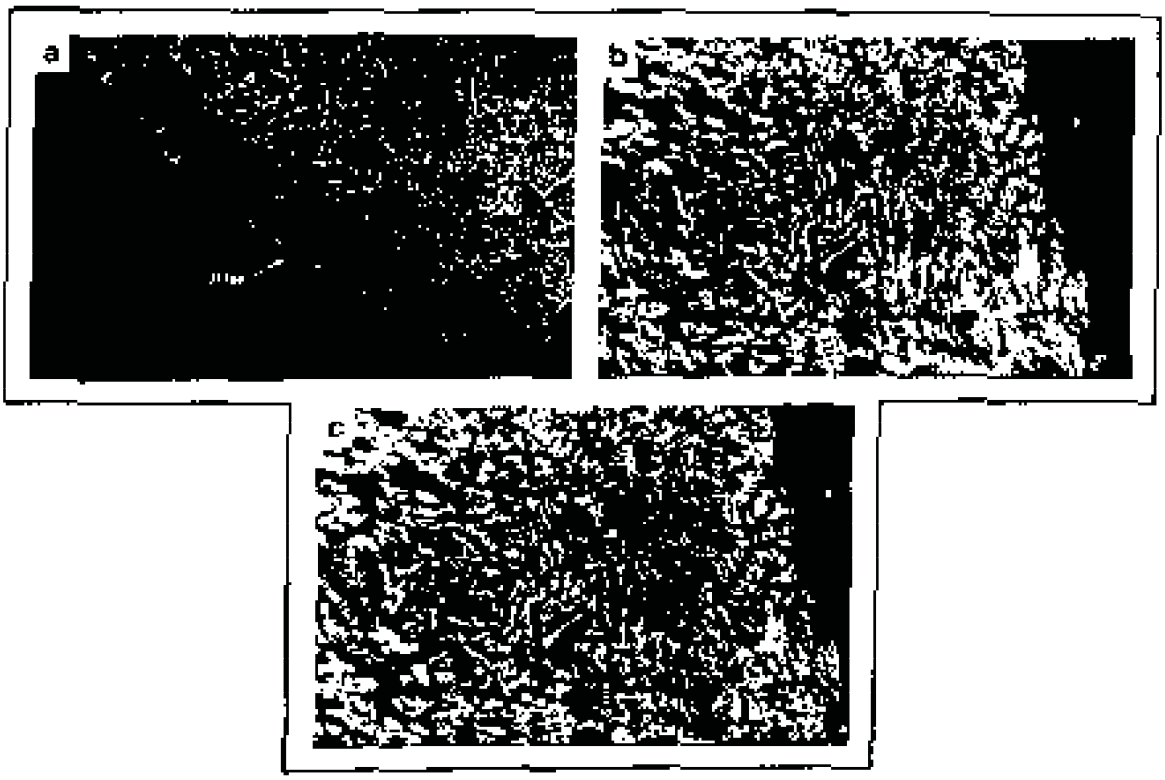

Figure 4.6 (ii) Cross-sectional electron micrographs of the porous rim of a three hour leached Alloy C catalyst after WGSR

a: *MAG x 500*
b: Zn mapping (MAG x 550)
c: Al mapping (MAG x 550)

The crystallite (dendritic) structures of the intermetallic compound are spread among the eutecticum of the three metals (Figures 4.5 (i) - (ii) and 4.6 (i) - ii)). Zinc and aluminium dissolve during alkali leaching to form highly dispersed copper enriched surface crystallites. Leaching does not change the general environment of the crystallites and it can be observed (Figures 4.5 (i) - (ii) and 4.6 (i) - (ii)) that the original particle volume (and shape) is retained and is therefore independent of leach time. There is no conclusive evidence in the unused catalyst of any mechanical structure collapse or damage

brought about by the leach action to produce a powdery material. Thus, changes in pore structure, pore volume, surface area etc. cannot be attributed to such an effect. However, crystallite shape changes with increasing leach time. Granular shapes are observed up to a leach time of 1.5 hours, after which longer times result in more elongated "needle like" crystallites.

Identification of the phases in Alloys C and D and their corresponding changes as a function of leach time was conducted using XRD analysis of the bulk. The phases identified in Alloys C and D, together with resultant leached catalysts before and after reactor testing are presented in Table 4.3 below.

Table 4.3 **Crystalline phases of Alloys C and D and their product Raney copper catalysts before and after reaction**

Sample	Extraction time (h)	Phases before reaction[a]	Phases after reaction[a]
Alloy C	-[b]	$CuAl_2$, Al, CuAl, (AlZn)[c], Zn	-
Alloy C	1.0	Cu_2O, CuO, $CuAl_2$, CuAl, (Zn)	Cu, Cu_2O, CuAl, CuO
Alloy C	1.5	CuO, CuAl, Cu_2O(tr)[d], $CuAl_2$(tr)	Cu, CuO, CuAl
Alloy C	2.0	CuO, CuAl, Cu_2O(tr) $CuAl_2$(tr)	Cu, CuO, CuAl
Alloy C	3.0	Cu_2O, CuO, CuAl	Cu, CuO, CuAl, Cu_2O
Alloy D	-	$CuAl_2$, CuAl, Al	-
Alloy D	1.5	CuAl, CuO, Cu_2O(tr)	CuAl, Cu, CuO, Cu_2O(tr)

[a] Phases listed in *approximate* order of abundance (from left to right)
[b] Dashes indicate not applicable
[c] Phase in brackets not conclusively identified
[d] (tr) = trace

The diffraction patterns of Alloy C and corresponding 1 and 3 hour leached catalysts before and after reactor testing are shown in Figure 4.7 (a) - (e).

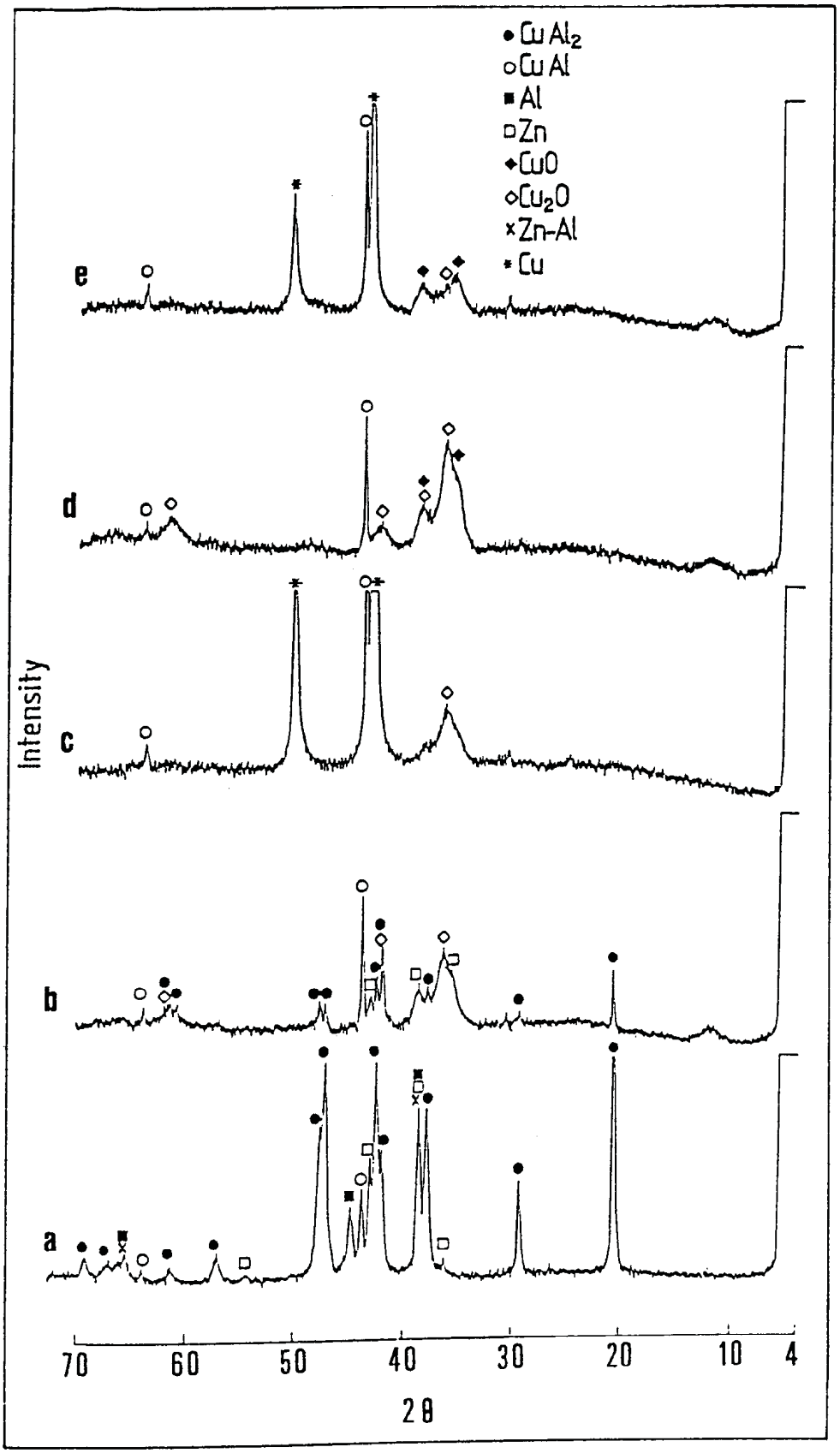

Figure 4.7 XRD patterns of fresh and used Raney copper catalysts produced from leaching Alloy C for various times

a: Alloy C, no extraction
b: 1.0 hour leach, before reaction
c: 1.0 hour leach, after reaction
d: 3.0 hour leach, before reaction
e: 3.0 hour leach, after reaction

The diffraction patterns of Alloy D and 1.5 hour leached catalysts before and after reactor testing are presented in Figure 4.8 (a - c).

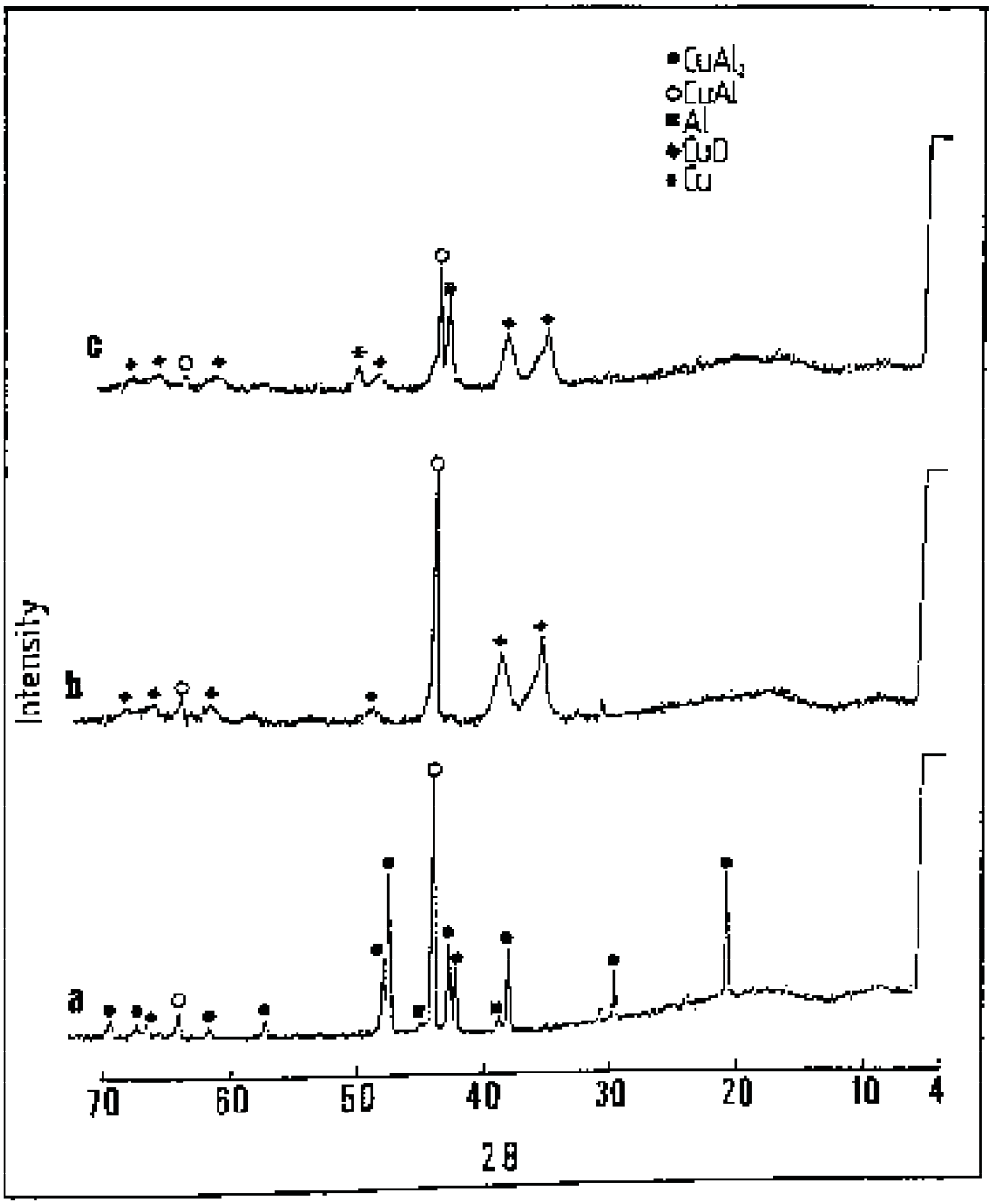

Figure 4.8 XRD patterns of fresh and used Raney copper catalysts produced from leaching Alloy D for 1.5 hours

a: Alloy D, no extraction
b: 1.5 hour leach, before reaction
c: 1.5 hour leach, after reaction

Only CuO could be identified from XRD patterns of the fresh co-precipitated and industrial ICI 53-1 catalysts.

The microstructures of Alloys C and D are consistent with predictions for quenched alloys made from the liquidus projection diagram (Chapter 2, Figure 2.1). Both alloys have the binary $CuAl_2$ phase as their primary precipitate. It is possible that this phase may be represented as $Cu(Zn)Al_2$ for Alloy C as it is known that the $CuAl_2$ phase can dissolve up to 2 - 3wt% Zn with little change in lattice parameters (12). The identity of the secondary precipitate(s) is determined by the alloy Zn level (13). Alloys C and D show well resolved patterns indicating the binary CuAl phase and an Al solution as secondary products. A larger abundance of the CuAl phase is seen in Alloy D due to its closer "proximity" to the CuAl phase constitution than that of Alloy C (see liquidus projection diagram, Chapter 2, Figure 2.1). It is well documented by Friedrich *et al.* (13, 14) that ternary Cu-Zn-Al alloys of similar compositions to those reported in Chapter 2, Table 2.1 contain a $Cu(Zn)Al_2$ phase in the form of grains surrounded by a second major phase, which is a AlZn solid solution. The former leaches to produce porous copper whilst the latter leaches completely leaving void spaces. Due to the complexity of the diffraction pattern for Alloy C (Figure 4.9) all possible AlZn peaks were masked by Al, which made it impossible to prove (or disprove) the existence of AlZn, however a solid Zn solution was clearly observed. No evidence of the ternary phases T = $Cu_5Al_3Zn_2$ and T' = Cu_3Al_3Zn (Chapter 2, Figure 2.1) previously identified by XRD in similar Cu-Zn-Al alloy compositions by Bridgewater *et al.* (4) were found. Also, the XRD analysis did not reveal the presence of α-brass which has been reported to be formed in Cu-ZnO catalysts for the WGSR (15).

(b) Development of catalyst structure

Examination of AA (Table 4.2) and EDAX (Table 4.3) data

together with SEM micrographs (Figures 4.2 (i) - (ii) - 4.6 (i) - (ii)) as well as XRD patterns (Figures 4.7 and 4.8), reveals that the morphology of Raney copper catalysts is produced by caustic leaching which proceeds in three stages. Friedrich *et al.* (14) also observed three distinct stages of Raney copper morphological development.

In the <u>first stage</u> (times up to 1.5 hours) leaching of the $CuAl_2$ phase and Al solid solution from Alloy D leads to the formation of a <u>fully extracted alloy</u> with copper containing traces of Al. Similarly, the aluminium and zinc content of Alloy C drops rapidly from initial levels, due to the leaching of intergranular Al and Zn solid solutions (together with binary AlZn), and the $Cu(Zn)Al_2$ grains of the outer layer. This stage corresponds to the *formation* of an "alloy-catalyst" interface in ternary Cu-Zn-Al alloys. Thus, the addition of Zn to the precursor alloy has the effect of slowing the rate of the leach reaction. In a study on the leach kinetics of alloys with varying initial alloy compositions Friedrich *et al.* (16) noted that introducing small amounts of Zn to the alloy (up to 10 - 15%) substantially increases the leaching rate, but addition of more Zn leads to a decrease in the leach rate. This phenomena derives from changes in the interface values for the activities of the diffusing species with hydroxide which in turn depends on alloy composition.

Interface boundaries were observed to cut across the phases present, leaching intergranular material at a uniform rate around the circumference of the "attack front". The majority of the $Cu(Zn)Al_2$ phase is evenly leached from the outer rim (see Figure 4.4 (i)), parallel to the particle boundary, to leave porous Raney copper. This result is consistent with the findings of Friedrich *et al.* (13) who reported that under similar conditions, the intergranular solidification products of alloys containing a minimum of 17wt% Zn leached at a <u>faster</u> rate than the $Cu(Zn)Al_2$ phase, for time periods of less than four hours. A significant observation was that for all alloys and leach times, the Al

associated with Cu in the CuAℓ phase, was resistant to caustic attack. Friedrich *et al.* (13) also observed the presence of an unidentified intergranular material which had not been leached near the reaction front. No reason for the decrease in reactivity of this material could be determined. Oxidised copper was the most abundant product formed by leaching and subsequent exposure to atmospheric oxygen. All fresh, air dried catalysts contained CuO, and in some cases also Cu_2O. After reaction, elemental Cu was predominant in all the Raney catalysts. Discharged catalysts were exposed to the atmosphere before XRD analysis, thus permitting the partial re-oxidation of copper observed. It is concluded that under WGS conditions, the active Raney catalyst phase is elemental copper.

Andreev *et al.* (10, 17) used XRD to identify "considerable amounts" of cuprous oxide, probably due to the oxidation of finely dispersed copper particles by oxygen from the leach solution, after being intensively stirred. The same authors used EPR to study the precursors of a low temperature co-precipitated catalyst and the surface layers of a leached granule. Due to the similarity in the spectral parameters of the two catalysts, it was concluded that the Raney catalyst contained Cu^{2+} ions in an oxide matrix, similar to the oxide catalyst obtained by co-precipitation. The authors XRD analysis (10) of leached material also showed the presence of complex hydrotalcite-like phases with the general formula of $Cu_xZn_{6-x}Aℓ_2(OH)_{16}CO_3$ regarded to be formed on the surface of the catalyst. Formation was considered to be enhanced by the suitable conditions at which leaching was carried out. Carbonates in the solution originated from impurities in the NaOH. Insufficient washing probably resulted in the presence of these phases in the catalyst product.

In the second stage of reaction (times of 2 - 3 hours) repeated analysis showed that there is an overall increase in bulk copper content, with increasing extraction time. The levels of Cu in the leached product (rim) remained

relatively constant after 1 hour, with a corresponding decline in Zn concentration. The Aℓ content in the leached product steadily increased (from a minimum of 6.2% at 1.5 hours to 11.2% after 3 hours) and remained at relatively high levels until the alloy core of the leaching particle was completely exhausted. This result is only consistent if there is a net transfer of Aℓ from the leaching intergranular solid solution to the $Cu(Zn)Aℓ_2$ phase leach residue. Previous studies (16) showed that the leach reaction is liquid diffusion controlled and involved the reprecipitation of oxidised species, particularly Zn, near the leaching front, as detailed in Section 4. No conclusive reason was presented, but Friedrich *et al.* (16) suggested that preferential Zn re-precipitation occurs because of the vast difference in solubilities of Zn and Aℓ in caustic solutions. This argument is however, subjective, and only applies to specific compounds of Zn and Aℓ. If, for example the precipitation product of Aℓ is hydrargillite, $Aℓ_2O_3.3H_2O$, and that of Zn is $Zn(OH)_2$, then the ratio of Aℓ to Zn solubility is 16:1 (16). This would mean that the dissolution of Aℓ from $Cu(Zn)Aℓ_2$ can deplete the OH^- activity to the point where Zn is precipitated. Bridgewater *et al.* (4) observed that after theoretically removing all Aℓ and Zn (from alloys with an Aℓ content ≥ 39 wt%, a Zn content between 13 - 15 wt% and Cu levels < 50 wt%) as calculated from the expected volume of hydrogen produced during reaction, elemental analysis still showed the presence of Aℓ and Zn. The authors concluded that both Aℓ and Zn re-precipitated during reaction, most likely as a result of the fall in pH at the centre of the catalyst particle due to the decrease of OH^- by reaction with Aℓ and Zn, and diffusional limitations upon the migration of OH^- from the bulk solution to the catalyst interior. This re-precipitation of Aℓ and Zn means that, under reactor operating conditions, the Raney copper will have Cu, ZnO and $Aℓ_2O_3$ present in the catalytically active zone (4). Andreev *et al.* (10) reported the formation of mixed hydrocarbonates on Raney copper which was considered to come from the participation of zincate and aluminate anions

from the solution. The high Aℓ content observed in alloys leached for 1.5 - 3 hours may also be attributed to the presence of alumina trihydrate which has been reported (18) to precipitate on the porous copper surface during the leaching and washing process. Alumina trihydrate is also known to decompose to alumina during the degassing of samples for surface area analysis.

In the third and **final stage** of reaction, the Aℓ content was lowered as the residual soluble metals were removed. It may be concluded that the nature of Raney copper catalysts derive from the phase constitution of their precursor alloys and subsequent morphological development which is sensitive to leach time.

(c) Leaching kinetics

The *extent* of reaction was determined by measuring the depth of leach attack on Alloy C particles as a function of time. The results are presented in Figure 4.9 below.

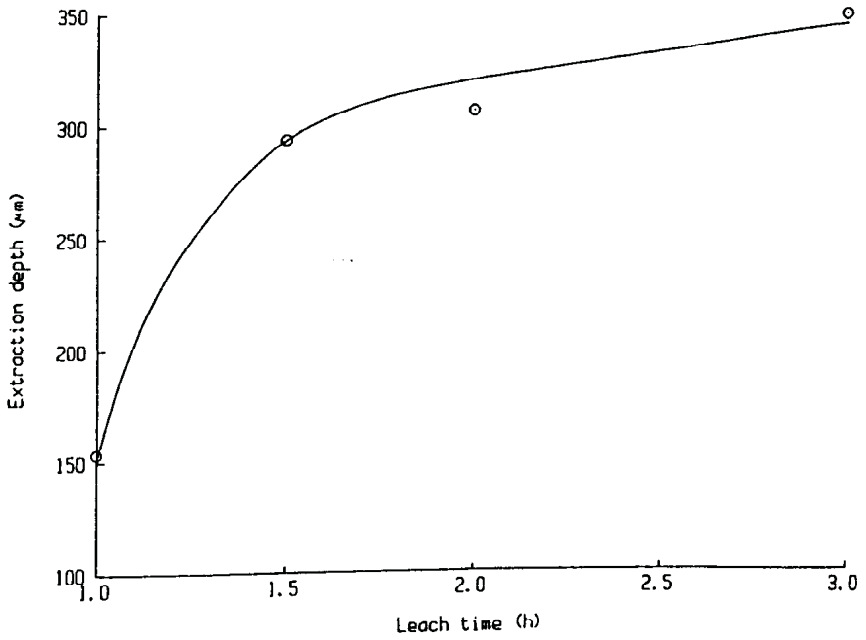

Figure 4.9 **Average diameter of reaction rim as a function of caustic leaching time**

The shape of the curve indicates parabolic leaching kinetics (16) and suggests that the process is *diffusion controlled*. Three possible mechanisms to rationalize this finding are: (i) solid-state diffusion in the reacted rim, (ii) diffusion within the alloy where copper (the noble metal) forms a continuous film at the alloy surface and selective dissolution of the active leachable metals is only possible by volume diffusion through the copper, and (iii) liquid phase diffusion. Friedrich *et al.* (16) found that Cu-Zn-Al alloys containing 50 wt% Al and approximately 0, 5, 10, 17, 26 and 33 wt% Zn displayed parabolic leaching kinetics with a selective dissolution mechanism, controlled by liquid phase diffusion through the product layer. Curry-Hyde *et al.* (19) applied the "shrinking core model" proposed by Levenspiel (20) to study the leaching kinetics of a 39 wt% Cu, 17.8 wt% Al, 43.2 wt% Zn alloy over a range of leachant temperatures and concentrations. The authors also determined that a satisfactory description of the kinetics of leach penetration into the alloy could be provided under most circumstances, by the expression for diffusion control represented below:

$$t = \tau [(X + (1-X) \ln (1-X)] \qquad - (4.1)$$

where:

$$\tau = \frac{(b_{Al}\rho_{Al} + b_{Zn}\rho_{Zn}) R^2}{4 D_{OH} (C_1(R) - C_1(r_c))} \qquad - (4.2)$$

and

$$X = 1 - \left(\frac{r_c}{R}\right)^2 \qquad - (4.3)$$

also:
- t = time (h)
- R = radius of pellet
- r_c = radius of unleached core
- ρ_{Al} and ρ_{Zn} = bulk concentrations of Al and Zn in the alloy ($gmol.cm^{-3}$)
- b = stoichiometric coefficient for the reaction of OH^- with Al or Zn ($b_{Al} = 1$ and $b_{Zn} = 2$)
- D_{OH} = effective diffusion coefficient of OH^-
- $C_1(R)$ and $C_1(r_c)$ = the concentrations of sodium hydroxide at the outside of the pellet and at the alloy-catalyst interface, respectively

The rate of leaching was found to be dependent on both temperature and concentration of the sodium hydroxide solution. A high concentration of $Zn(OH)_4^{2-}$ in the leached $Cu(Zn)Al_2$ grains at the product interface was reported (19) to result in a significant deposition of $Zn(OH)_2$. Secondary dissolution of $Zn(OH)_2$ from the porous copper was observed to occur away from the interface. The process was shown to be first order with respect to hydroxyl ion concentration and accurately described by a Langmuir-Henshelwood adsorption model. Liquid phase diffusion was sufficiently rapid to support the mass transfer rates required for both the leaching and secondary dissolution processes.

(d) Development of surface structure

It has been shown recently (21) that incomplete extraction of Cu-Zn-Al alloys with caustic solution can lead to "marked changes" in surface and pore morphology. Since heterogeneous catalysis is a surface phenomenon, the determination of surface properties play a large part in catalyst characterisation. The high surface area and extensive porosity of Raney copper catalysts (2) made it possible to use the classical nitrogen adsorption/desorption technique to analyse the BET surface area, total pore volume and pore radii distribution of these catalysts. Copper surface area and crystallite size were determined according to procedures outlined in Chapter 2, Section 2.5.2 and are a measure of reproducibility, rather than of correspondence to absolute values.

The nitrogen isotherms for Raney catalysts produced by leaching Alloy C for 1, 1.5, 2 and 3 hours showed a **Type A** hysteresis loop (22) which is representative of cylindrical capillary shapes, as would be expected for the "striated" needle-like nature of the leached copper product. The BET and copper surface areas, together with crystallite diameter and copper dispersion are presented in Table 4.4 for catalysts derived from Alloys C and D, as well as the ICI 53-1 industrial catalyst and a co-precipitated WGS catalyst.

Table 4.4 **Surface area, crystallite diameter, and dispersion of fresh and used Raney copper catalysts of varying copper leach times**

Sample	Extraction time (h)	S_{BET} ($m^2.g^{-1}$)	S_{Cu} ($m^2.g^{-1}$)	Copper Crystallite Diameter (Å)	Copper Dispersion (%)
Alloy C	1.0	27.0 (21.5)[a]	15.7 (4.6)	297 (1003)	5.3 (1.8)
Alloy C	1.5	33.4 (20.3)	16.9 (2.9)	294 (780)	6.6 (2.4)
Alloy C	2.0	32.8 (19.0)	15.8 (10.1)	324 (514)	5.8 (3.7)
Alloy C	3.0	28.2 (22.2)	13.7 (9.9)	415 (572)	4.5 (3.3)
Alloy C	19.5	10.2 -[b]	7.8 -	750 -	2.6 -
Alloy D	1.5	20.0 (15.8)	10.2 (6.9)	557 (841)	3.4 (2.4)
ICI 53-1		81.6 (80.7)	8.2 (7.4)	212 (238)	9.2 (8.1)
Precip.		85.9 (83.2)	5.3 (7.5)	157 (143)	12.2(13.5)

[a] Results in brackets for used catalysts
[b] Dashes indicate not measured

The corresponding pore volumes and mean pore radii for the catalysts described above are shown in Table 4.5.

Table 4.5 **Pore volume and mean pore radii of fresh and used Raney copper catalysts of varying leach times**

Sample	Extraction time (h)	Pore volume ($cm^3.g^{-1}$)	MPR[a] (Å)
Alloy C	1.0	0.062 (0.058)[b]	56.9 (53.9)
Alloy C	1.5	0.082 (0.08)	68.7 (75.5)
Alloy C	2.0	0.197 (0.141)	121.2 (184.4)
Alloy C	3.0	0.313 (0.187)	260.6 (324.8)
Alloy C	19.5	0.026 -[c]	99.5 -
Alloy D	1.5	0.194 (0.164)	122.7 (145.8)
ICI 53-1		0.257 -	69.4 -
Precip.		0.471 -	203.3 -

[a] MPR = Mean Pore Radii
[b] Results in brackets for used catalysts
[c] Dashes indicate not measured

Pore development of the Raney copper system is of interest as it provides information on the manner in which the catalyst is formed (2). The compositional and phase constitutional variables in the precursor alloys are known (2) to significantly influence the pore geometry and consequently the surface area of their product catalysts. From Table 4.5 it can be seen that the **pore volume** increased as the Aℓ and Zn content of Alloy C was depleted, whilst the removal of residual Aℓ and Zn after 19.5 hours leaching resulted in the partial elimination of these pores. **Pore radii** (Table 4.5) and **copper crystallite size** (Table 4.4) increased with increasing extent of leach reaction, which qualitatively confirms the trend. Also, a decrease in pore size after core extraction confirmed that pore elimination takes place as a result of the removal of **residual** metals. The pore size is expected to increase with time as the soluble core elements are progressively removed (14). Friedrich *et al.* (14) observed that the leaching reaction must be accompanied by *microstructural re-arrangement* in which the pore and crystallite size are interdependent on each other. The copper crystallite size through the leached layer of Cu-Aℓ and Cu-Zn-Aℓ pellets (5.4 mm x 4.7 mm) was shown (9) to increase in size with distance from the interface, until a limiting value at the external surface was observed. This profile demonstrated the significance of copper re-arrangement, especially in large particles where the phenomenon was used to explain the observed changes in surface area and pore size distribution of the catalyst pellets. The re-arrangement was reported (9) to be due to the dissolution of copper from faults within the copper structure which had a high radius of curvature and followed by re-precipitation on adjacent copper rods where the radius of curvature was lower. Tomsett *et al.* (23) studied the extraction of Cu-Aℓ alloys and reported that the mean pore size increased with particle size. The control of pore spacings, and hence pore sizes was attributed to solid-state diffusion within the alloy, driven by a chemical potential gradient resulting from the leach reaction. Onuoha *et al.* (21)

showed that this description was also applicable to the formation of partially leached Cu-Aℓ alloys, where pore size increased with increasing thickness of active rim. A total pore volume which increases with leach time implies that the average pore radius must also increase (14), which was observed (Table 4.5).

Total BET surface areas reach a maximum after about 1.5 hours leaching time, and then follow a slight decline. A maximum in surface area after approximately 1 - 2 hours leaching has been observed by many researchers, both for leaching Cu-Aℓ alloys (21) and Cu-Zn-Aℓ alloys (24). Onuoha *et al.* (21) describe the maximum surface area as a result of the monotonical increase in both pore volume and pore radius with the extent of the reaction whilst Tomsett *et al.* (24) draw a connection between the concentration of alumina from the deposition of alumina trihydrate and the high surface area. The copper surface area and dispersion expectedly decrease with increasing crystallite size. At all leach times, copper surface dispersion is more efficient for the industrial and co-precipitated catalysts. Raney copper surface areas and crystallite diameter are plotted as a function of leach time in Figure 4.10.

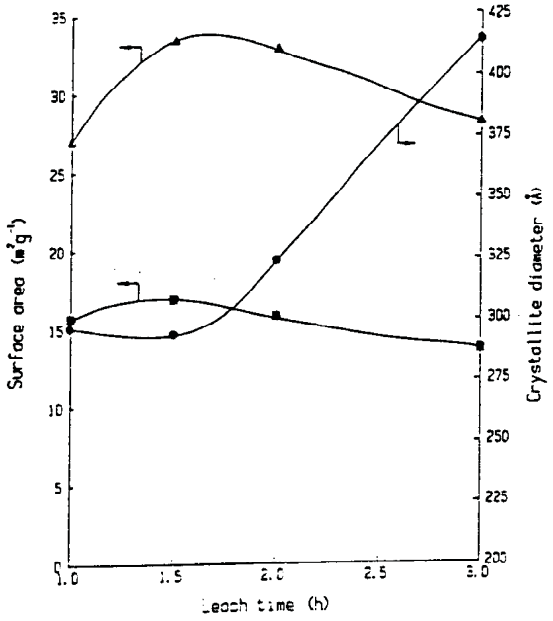

Figure 4.10 **Surface area and crystallite diameter of Raney copper catalysts produced from Alloy C as a function of leach time**

▲ = BET surface area; ■ = Copper surface area;
● = Crystallite diameter

Leaching for a long time results in wider pore openings (Table 4.5) reducing the likelihood of pore blockage while still allowing access of reactants to the high specific copper surface area in the interior of the particle. An optimal leach depth range (approximately 150 - 300 μm, see Figure 4.9) for the best predicted catalyst performance occurs after only 1 - 1.5 hours leaching (for the reported conditions, see Section 4.2), when (copper) surface area is a maximum and crystallite diameter a minimum. Pore radii, although at a minimum at this leach time, are still large enough to support mass transfer effects and compare to sizes present in co-precipitated and ICI 53-1 catalysts. For leach times greater than the optimum, both the BET and copper surface areas gradually decrease even though the volume of leached material increases (Table 4.5). It has been shown that the increase in crystallite size ("coarsening") with leach time ("aging"), results in the largest pores being found at the surface, which has important implications for the activity and stability of the Raney copper catalysts.

(e) Thermometric analysis of partially leached Raney copper catalysts

Using DSC, the reduction procedure under 5% H_2/N_2 was simulated in order to supplement the structural information obtained by XRD. The catalyst samples were heated from ambient to 300°C at a rate of 5°C/min and a gas flow of 30 ml/min. Heat flow was monitored during the run (Chapter 2, Section 2.5.1). DSC curves for the Raney copper catalyst produced from leaching Alloy C for 1, 1.5, 2 and 3 hours and Alloy D for 1.5 hours under standard conditions (Chapter 2, Section 2.1.1) together with the curve for the industrial ICI 53-1 catalyst are shown in Figure 4.11.

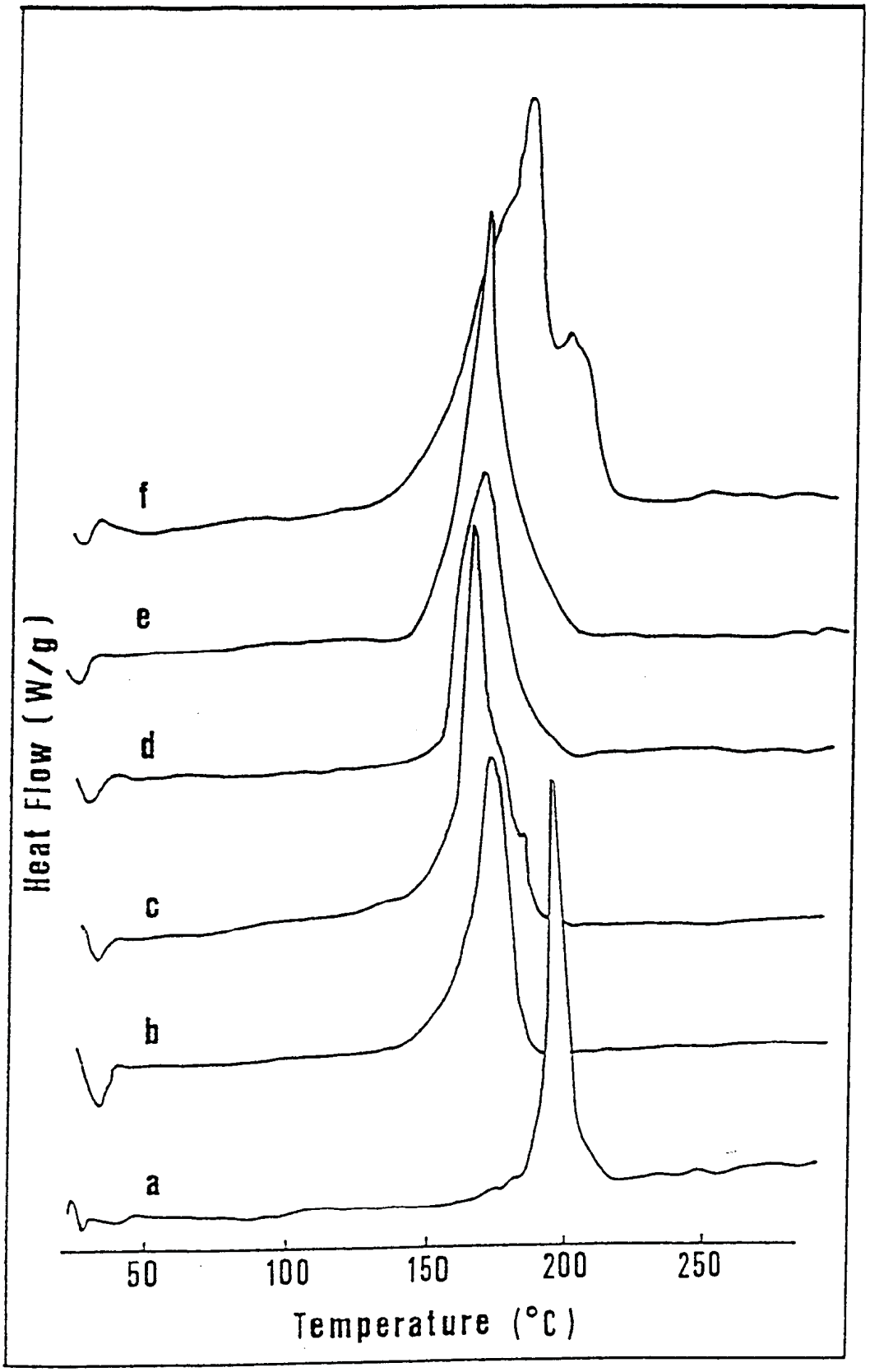

Figure 4.11 DSC curves of an industrial low temperature shift catalyst and Raney copper catalysts produced from leaching Alloy C for various times

a: ICI 53-1 catalyst
b: Alloy C, no extraction
c: 1.0 hour leach
d: 1.5 hour leach
e: 2.0 hour leach
f: 3.0 hour leach

From Figure 4.11 it can be seen that reduction involved a single major exothermic phase change between 165 and 220°C. Pure Cu_2O and CuO powdered samples were observed to reduce over a similar temperature range (165-225°C) under the same experimental conditions. The more complex exothermic peak of 1 and 3 hour leached Alloy C catalysts is probably due to the reduction of Cu(I) and Cu(II). Both oxidation states of copper are significantly present in the mentioned catalysts (see Table 4.3). Copper oxide is also reported (3) to be reduced to elemental copper during activation of the ICI 53-1 catalyst. Rasulic *et al.* (25) observed an exothermic DSC peak for the reduction of CuO in hydrogen. Maximum peak temperature was not reported, but a temperature interval from 140 to 200°C was scanned. The DSC results are consistent with the XRD analysis (Figures 4.7, 4.8 and Table 4.3) which showed that oxidised copper was reduced to elemental copper during the activation procedure.

Since it is known (26) that Raney copper catalysts are susceptible to sintering during reduction, it was considered useful to investigate the influence of the reduction conditions chosen for catalyst reactor testing (see Chapter 2, Section 2.2.1) on the active Raney copper surface area under various reducing atmospheres. Consequently investigations by DSC at a temperature climb rate of 5°C/min in currents of pure H_2, CO and 5% H/N_2 (at a flow rate of 30 ml/min) were carried out using a 1.0 hour leached (Alloy C) Raney catalyst with small sample weights up to 0.15 mg, arranged as a fine layer to ensure copper reduction was practically possible in the whole mass of sample. Table 4.6 shows the copper reduction energies obtained in the various atmospheres together with corresponding active catalyst copper surface areas (determined using a N_2O pulse flow technique described in Chapter 3).

Table 4.6 **Energy changes and corresponding copper surface areas associated with the reduction of a Raney copper catalyst in various atmospheres**

Alloy C leach time (h)	Reducing atmosphere	Copper reduction energy ($J.g^{-1}$ cat.)	S_{Cu} ($m^2.g^{-1}$)
1.0	5% H_2/N_2	189.7	15.7
1.0	Pure H_2	215.3	12.1
1.0	Pure CO	493.6	9.8

Significant loss of surface area is seen when pure hydrogen or carbon monoxide is used as reductant (Table 4.6). The greatest loss in surface area corresponds to the highest generated reduction energy in the bed, inferring that sintering of the Raney copper was responsible for loss of surface area.

Reactions for the reduction of CuO in H_2 and CO have been reported (26) as:

$$CuO + H_2 \rightleftharpoons Cu + H_2O \qquad \Delta H(573K) = -88.2\,kJ.mol^{-1} \qquad (4.4)$$

$$CuO + CO \rightleftharpoons Cu + CO_2 \qquad \Delta H(573K) = -153.7\,kJ.mol^{-1} \qquad (4.5)$$

The greater exothermicity of Reaction 4.5 accounts for the higher reduction energy associated with carbon monoxide, and consequently the higher degree of sintering. Using the same reducing gases, Chongzheng *et al.* (26) also observed that reduction with CO resulted in the greatest loss of total surface area, which corresponded to the highest measured temperature rise. Raney copper catalysts showed no loss of surface area (26) as a consequence of the GHSV of reducing gas (5% H_2/N_2). The authors concluded that

sintering at higher temperatures was responsible for decreased total catalyst surface area. Recently (27) an experimental dynamical equation was used in an attempt to explain the continued loss of Raney copper surface area (enhanced at higher reducing temperatures) with increasing time of exposure to hydrogen.

The results show that under the stated reduction conditions (Chapter 2, Section 2.1.1) reduction in 5% hydrogen in nitrogen maximizes the active copper surface area of the Raney copper catalysts.

From the characterisation results it may be concluded that the phase composition of Raney copper catalysts is similar to that reported (in Chapter 1) and observed for a co-precipitated and an industrial WGS catalyst under operating conditions.

4.3.2 Activity and stability

(a) Activity

Partially leached Raney copper catalysts consist of an extracted rim of active material and a core of unextracted alloy. Although this core does not provide catalytic activity, it does contribute to the composite mass of the catalyst particle. The bulk density of a Raney catalyst particle of unit volume decreases as a function of increasing leach time (Table 4.7) and decreasing alloy copper content (Table 4.8). Hence careful interpretation of activity data based on the mass of Raney catalysts with varying alloy composition and/or extraction depth must be exercised.

Table 4.7 The bulk density of Raney copper catalysts as a function of leach time

Sample	Extraction time (h)	Density ($g.ml^{-1}$)
Alloy C	1.0	1.5
Alloy C	1.5	1.4
Alloy C	2.0	1.34
Alloy C	3.0	1.03
ICI 53-1		0.97*
Precipitated		1.0

* Reported bulk density (3) = $0.95 kg.l^{-1}$

Table 4.8 The bulk density of Raney copper catalysts as a function of alloy composition

Alloy (nominal wt%)	Extraction time (h)	Density ($g.ml^{-1}$)
Cu(43) Zn(18) Al(30)	1.0	1.73
Cu(35) Zn(15) Al(50)	1.0	1.5
Cu(25) Zn(25) Al(50)	1.0	0.88
Cu(10) Zn(40) Al(50)	1.0	0.84

The initial activities of the partially leached catalysts of Alloys C and D together with the industrial ICI 53-1 catalyst and a co-precipitated variation (see Section 4.2) are presented in Table 4.9. Specific activities are expressed as the rate (per hour) of moles of carbon monoxide converted as a function of: volume of catalyst particles (Rate a), composite (total) mass of catalyst particles (Rate b), specific copper surface area (Rate c) and BET surface area (Rate d).

Table 4.9 Specific activities of Raney, co-precipitated and industrial catalysts[a]

Sample	Extraction time (h)	Rate (a) ($mol_{CO}/ml/h$) x 10^{-3}	Rate (b) ($mol_{CO}/g_{composite}/h$) x 10^{-3}	Rate (c) ($mol_{CO}/m^2_{Cu}/h$) x 10^{-4}	Rate (d) ($mol_{CO}/m^2/h$) x 10^{-6}
Alloy C	1.0	3.44	2.30	1.47	8.50
Alloy C	1.5	3.41	2.43	1.44	7.29
Alloy C	2.0	3.44	2.58	1.63	7.86
Alloy C	3.0	3.29	3.21	2.34	11.37
Alloy D	1.5	3.37	2.92	2.86	14.61
ICI 53-1		3.06	3.19	3.84	3.86
Precip.		2.94	2.94	5.55	3.43

[a] Temperature = 200°C; Total GHSV = $1000 h^{-1}$; Dry gas composition = 10% CO/90% N_2; CO:H_2O = 1:22.5; Catalyst Volume = 2 ± 0.1ml

Expressing activity as a function of constant catalyst volume (Rate a) has the advantage of demonstrating that "particle for particle" Raney copper catalysts extracted from 1 - 3 hours are more active than the industrial and co-precipitated catalysts. As the catalyst volume required determines the type and size of convertor needed for a particular catalyst (28), Raney catalysts may present important economical advantages. Raney copper activity (Rate a) decreases with decreasing copper surface areas and increasing crystallite growth (Table 4.4) as expected. Activity based on the composite mass of the Raney catalyst (Rate b) highlights the variable density phenomenon. Increasing the extent of alloy extraction decreases the catalyst density with a corresponding overall increase in the activity based on composite mass. A comparison of the activities (Rate b) of catalysts with similar bulk densities (Table 4.7) indicates that on a mass basis the fully extracted 3 hour leached Raney copper catalyst (of lowest volume based activity) displays a higher activity than both the industrial and co-precipitated catalysts.

Some authors (14) have attempted to circumvent the variable density problem by expressing activity (for methanol synthesis) in terms of a theoretically calculated mass of "rim material" since the catalyst activity was suggested to correlate with the copper rim. This method also involves a large number of simplifying assumptions (21). Further, this contrasts with a fundamental principle of evaluating catalyst performance, which requires that testing (and by inference data processing) should be the same on a laboratory (micro) scale as in a full-scale (macro) reactor (28). In this thesis it is proposed that meaningful comparisons between potential catalytic systems must be made considering the entire catalyst particle.

The activities (Rate c) of Raney copper catalysts expressed in terms of specific copper surface area are low in comparison to the industrial and co-precipitated catalysts as a result of the high density, copper rich core which ensures a low percentage active metal dispersion (Table 4.4). However, from Table 4.9, it can be seen that all Raney copper catalysts evaluated showed a higher total surface area efficiency (Rate d), than the industrial and co-precipitated alternatives. This result is consistent with the findings of Andreev et al. (10) who also noted that the productivity per unit surface area of a Raney catalyst was significantly higher than that of a low-temperature co-precipitated oxide catalyst over a large interval of studied flow rates, with an inlet carbon monoxide concentration of 12.5%. Based on an evaluation of the data in Table 4.9 the competitively high initial activities of Raney copper catalysts for the WGSR validated a comprehensive study of the system.

(b) Stability

Andreev et al. (10) observed that operating Raney copper catalysts for the WGSR at temperatures which caused condensation of water vapour onto the catalyst surface did not impede the performance of the catalyst or change its

mechanical strength. However, a literature survey has confirmed that no long term activity studies have as yet been conducted on the use of Raney copper catalysts for the WGS reaction. Friedrich *et al.* (2) noted that Raney copper for methanol synthesis is resistant to sintering in the short term, and postulated a minimal loss in activity with time-on-stream due to the unique catalyst morphology. No detailed explanations were given for this proposal.

A series of Raney copper catalysts (prepared from Alloy C) were investigated for long term stability in the WGSR, and the results are shown in Figure 4.12. Specific activity for catalyst stability determination was based on the mass of catalyst copper content as it is independent of changing bulk and surface structure during reaction and therefore permits a meaningful comparison between catalysts.

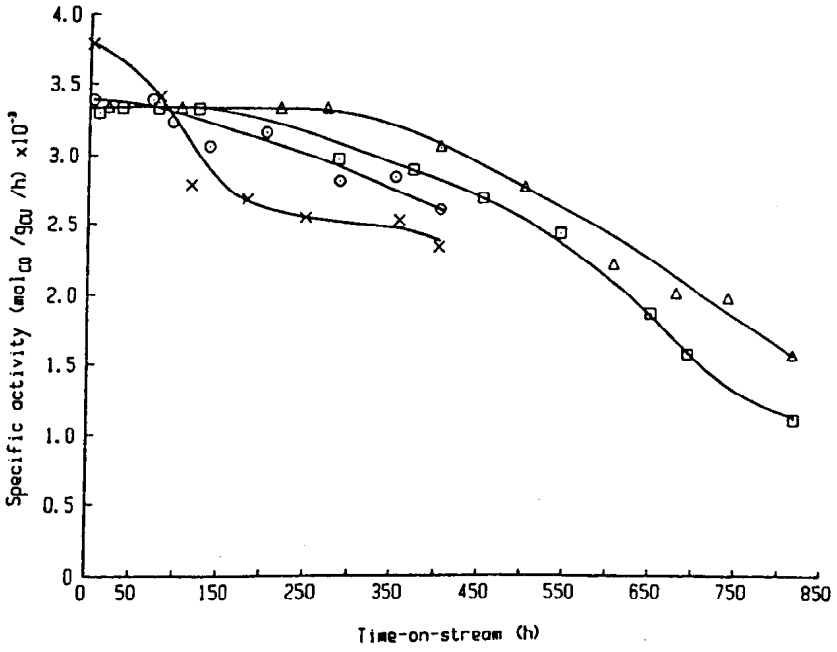

Figure 4.12 **Stability of various Raney copper catalysts as a function of Alloy C leach time[a]**

△ = 1.0 hour leach; ⊡ = 1.5 hour leach;
⊙ = 2.0 hour leach; X = 3.0 hour leach

[a] Temperature = 200°C; Total GHSV = 1000 h^{-1};
Dry gas composition = 10% CO/90% N_2; CO:H_2 = 1:22.5;
Catalyst Volume = 2 ± 0.1 ml

It can be seen from Figure 4.12 that the activity of the Raney coper catalysts had decreased significantly after 850 hours-on-stream. In comparison, the industrial ICI 53-1 catalyst showed a decrease of only 0.9% whilst no change in activity was observed for the co-precipitated catalyst over the same time period. No significant levels of sulphur or carbon were present in the used catalysts (as determined in a LECO HF 100 Induction Furnace). Notable decreases in the total surface area (Table 4.4) of Raney copper catalysts were, however, observed after the shift reaction. The decrease in availability of surface area occurs as a result of significant increases in copper crystallite size confirmed by dramatic decreases in specific copper surface areas. The decline in Raney copper activity is associated with the apparent decrease in copper surface area (Table 4.4). Behaviour of this nature during catalytic reaction is characteristic of sintering. Through sintering, the (active) surface metal dispersion is decreased by increasing the average size of the crystallites (30). The copper surface area and average crystallite diameter of the industrial ICI 53-1 and co-precipitated catalysts remain approximately constant during reaction, hence explaining the catalysts sustained stability. Sintering in Raney copper catalysts is not completely unknown. Chongzheng *et al.* (26, 27) reported that these catalysts are particularly susceptible to sintering in pure H_2 and CO environments during reduction. Our results reported in Section 4.3.1(e) confirmed the authors conclusions.

Analysis of the electron micrographs of the <u>surface</u> of 1 and 3 hour leached catalysts after WGSR (Figures 4.3 (i) and (ii)) shows that for both leach times the porous nature of the surface which was evident from leach action before reaction (Figures 4.2 (i) and (ii)) is no longer noticeable, even at high magnification. However, <u>cross-sectional</u> electron micrographs clearly revealed the growth of copper residue during reaction (Figures 4.5 and 4.6 (i) and (ii)) of 1 and 3 hour leached catalysts. "Islands" of high density copper crystallite growth are apparent

throughout the diameter of the leached rim. Prolific sintering of copper in the rim caused slight shrinkage to occur. For example, the average decrease in rim diameter of the 1 hour leached particle is 33%. The integrity of the rim remained unchanged, and no evidence of structural collapse was evident. The mean pore radii (Table 4.5) of the Raney copper catalysts increased upon sintering as predicted by Onuoha *et al.* (21). An increase in the size of large pores was observed by Chongzheng *et al.* (26) during reduction. Extensive reduction in pure hydrogen led to an almost complete elimination of these pores. The authors considered that pore size was governed by sintering during reduction. The lack of surface porosity in used Raney catalysts is consistent with this observation. An increase in mean pore radii is accompanied by a decrease in pore volume, the effect of which is more significant at long leaching times. The change in rim structure with extent of leach provides the explanation of this trend. Long, parallel, needle-like dendrites of the 3 hour leached catalysts provide a larger pore volume than the shorter, random orientated dendrites of the 1 hour leached catalyst. From Figure 4.6 (ii) it can be seen that a complete breakdown and randomization of the needle-like structure takes place with sintering, substantially decreasing the volume of the pores.

Raney copper catalyst stability (Figure 4.12), decreases with increasing leach time. It has been reported in Chapter 1, Section 1.4.1) that alumina together with zinc oxide may stabilize the copper crystallites of co-precipitated catalysts against thermal sintering. Analysis of the AA data (Table 4.1) of catalysts before and after reaction shows that taking into account experimental variation, no significant loss of either Zn and Aℓ takes place during reaction. Cross-sectional elemental mapping (Figure 4.6 (i)) of the rim of a one hour leached Raney catalyst after reaction reveals no concentration effects of support materials. It would therefore seem unlikely that sintering of copper crystals occurs as a consequence of the

migration of Zn or Al under WGS conditions. Raney copper stability for the WGSR decreases with decreasing catalyst zinc content. An increase in the rim Al content from re-precipitation (after 2 hours leaching) has no effect on maintaining high catalyst activity. It is also evident that decreases in bulk and rim Zn content of less than 1wt% result in observable changes in Raney copper stability.

A comparison of the XRD phases of the fully extracted fresh 3.0 hour leached Alloy C catalyst and the 1.5 hour leached Alloy D catalyst with similar bulk copper contents (84.6 and 84.7% respectively, Table 4.1) shows that the dominant leach resistant CuAl phase in Catalyst D does not effectively contribute to the specific copper surface area (Table 4.4). The higher copper surface area of Catalyst C resulted in a higher initial WGS activity as shown in Figure 4.13.

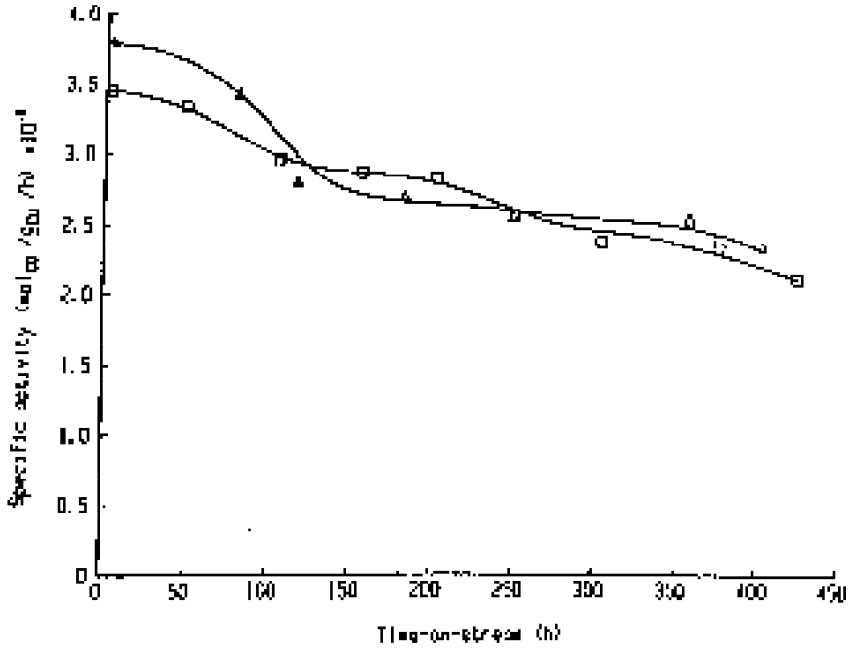

Figure 4.13 Stability of a ternary Raney catalyst (C) and a binary Raney catalyst (D) of similar bulk copper contents*

Δ = Alloy C:3.0 hour leach; □ = Alloy D:1.5 hour leach

* Temperature = 200°C; Total GHSV = 1000 h^{-1}; Dry gas composition = 10% CO/90% N_2; CO:H_2O = 1:22.5; Catalyst Volume = 2 ± 0.1ml

Both catalysts showed similar deactivation profiles and activity losses (± 38%) after 400 hours-on-stream, indicating no stabilization effect from the bulk 1.8 ± 1.5 wt% zinc content in the 3 hour leached Alloy C catalyst. No zinc was observed from EDAX analysis (detection limit of approximately 1%). Hence, residual zinc, if any, is most likely positioned deep within the particle or well dispersed, consequently exerting no stabilizing influence on the surface structure. The ion implanted results presented in Section 4.5 support this conclusion by showing that small concentrations of zinc concentrated near the catalyst surface contribute towards surface area stabilization.

4.3.3 Ion implantation

The results from Section 4.4 suggested that only small amounts of zinc were necessary to minimize the sintering of Raney copper crystallites during the WGS reaction. Implanting varying concentrations of Zn^+ ions into the subsurface rim region of a one hour leached Cu(50) Aℓ(50) alloy was employed to ascertain the stabilizing effect of a localized concentration of Zn^+ ions.

Based on the EDAX determined rim copper and aluminium concentrations of 84.99 wt% and 8.34 wt% respectively, the trajectory of 50 KeV Zn^+ ions into the catalyst was simulated using the TRIM-89 Version 5.1 computer program. The projected range and distribution of the zinc implanted ions are shown in Figure 4.14.

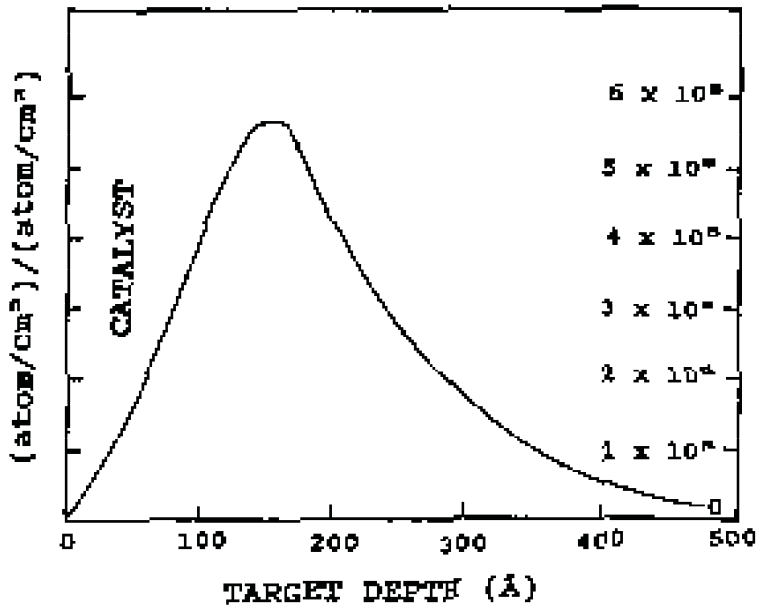

Figure 4.14 Projected range and distribution of zinc ions into a Raney copper catalyst

From Figure 4.14 it can be seen that a Guassian distribution of Zn^+ ions with a mean range of 174Å is predicted. As the smallest calculated Raney copper crystallite diameter is 1.7 times greater than the mean depth of Zn^+ penetration (Table 4.4), it is feasible to assume that the implanted zinc concentration may influence the surface structure. Table 4.10 shows the ICP-MS (Chapter 2, Section 2.5.1) determined Zn^+ ion dosages of Samples 2 - 5 after taking into consideration the non-implanted catalyst's average Zn background concentration which was equivalent to 8.5×10^{-3} wt%. Dosages are expressed in terms of an average total surface area (A) of the non-implanted catalyst. As a control, inert Kr^+ (of closest atomic mass to Zn^+) was implanted to a similar theoretical dosage (calculated from Equation 2.6) observed for the Zn^+ implanted catalysts. Noble gases have previously been implanted into catalysts in order to separate (any) catalytic activity as a result of radiation damage from that of the implanted ion under consideration.